Allergologia et immunopathologia
Sociedad Española de Inmunología Clínica, Alergología y Asma Pediátrica
www.all-imm.com

ORIGINAL ARTICLE

OPEN ACCESS

Effect of miR-1 and miR-126-5p in BCL2 and PIK3R2 regulation in apoptotic signaling during ST-elevation myocardial infarction

Arshia Mehmood[a,b†], Almas Muhammad Arshad[a†], Awais Altaf[a,c*], Tahir Maqbool[a], Hafiza Saba Safdar[a], Muhammad Faisal[d], Madeeha Shahzad Lodhi[a,c*], Nawal Al-Hoshani[e], Maher S. Alwethaynani[f], Shaza N. Alkhatib[g], Omniah A. Mansouri[h], Hanan Abdulrahman Sagini[h]

[a]*Institute of Molecular Biology and Biotechnology, The University of Lahore, Lahore, Pakistan*
[b]*Department of Biochemistry, Bakhtawar Amin Medical and Dental College, Multan, Pakistan*
[c]*Faculty of Health Sciences, Equator University of Science and Technology, Masaka, Uganda*
[d]*Department of Biotechnology, Institute of Plant Breeding and Biotechnology, MNS-University of Agriculture, Multan, Pakistan*
[e]*Department of Biology, College of Science, Princess Nourah bint Abdulrahman University, PO Box 84428, Riyadh 11671, Saudi Arabia*
[f]*Department of Clinical Laboratory Sciences, College of Applied Medical Sciences, Shaqra University, Alquwayiyah, Riyadh, Saudi Arabia*
[g]*Department of Biological Sciences, College of Sciences and Arts Khulais, University of Jeddah, Jeddah, Saudi Arabia*
[h]*Department of Biological Sciences, College of Science, University of Jeddah, 21493, Jeddah, Saudi Arabia*

[†]Joint first authorship (Contributed equally to this work)

Received 21 August 2025; Accepted 30 October 2025
Available online 1 January 2026

KEYWORDS
coronary artery disease;
myocardial infarction;
ST-elevation myocardial infarction;
cardiac troponin T;
BCL2;
PIK3R2;
miR-126-5p

Abstract
ST-elevation myocardial infarction (STEMI) involves the complete blockage of a coronary artery, leading to severe cardiac damage and high mortality. miR-1 promotes cardiomyocyte apoptosis by downregulating the anti-apoptotic protein BCL2, while miR-126-5p negatively regulates *PIK3R2* by activating the PI3K/Akt pathway. The expression of these miRNAs correlates with *BCL2*, *PIK3R2*, and high-sensitivity cardiac troponin T (hs-cTnT) in patients and controls, highlighting their role in apoptosis and myocardial injury. This study aimed to compare serum levels of miR-1, *BCL2*, microRNA-126-5p (miR-126-5p), Phosphoinositide-3-Kinase Regulatory Subunit 2 (*PIK3R2*), and cTnT in patients and controls. The association of miR-1 with *BCL2* and miR-126-5p with *PIK3R2* in STEMI patients was analyzed using ELISA and statistical analysis. Results showed a substantial increase in *BCL2* levels in STEMI patients (128.01 ± 137.19) compared to controls (40.65 ± 20.92), and a decrease in miR-1 levels in STEMI patients (31.35 ± 68.89) compared to controls (43.43 ± 31.28). Similarly, the *PIK3R2* and miR-126-5p levels among cases and controls were 228.55 ± 127.4 and 0.17 ± 0.32, respectively,

***Corresponding authors:** Madeeha Shahzad Lodhi and Awais Altaf, Institute of Molecular Biology and Biotechnology, The University of Lahore, Lahore, Pakistan. *Email addresses*: madeeha.shahzad@imbb.uol.edu.pk; awaisaltaf362@yahoo.com

https://doi.org/10.15586/aei.v54i1.1520

showing a significant difference between patients and controls. Statistical analysis revealed that the expression levels of miR-1 and miR-126-5p are significantly different between controls and patients (p-value < 0.05), demonstrating a strong association with the prognosis of ST-elevation myocardial infarction. Moreover, a strong correlation was observed between BCL2 levels and PIK3R2 levels (p-value < 0.05) among STEMI patients. These results establish a profound diagnostic profile for STEMI using miR-1 and miR-126-5p and highlight the functional importance of these miRNAs in angiogenesis by targeting the *BCL2* and *PIK3R2* proteins.

Introduction

Acute coronary syndrome (ACS) refers to the severe forms of myocardial infarction (MI), including non-ST-segment elevation, ST-segment elevation myocardial infarction (STEMI), and unstable angina (UA).[1] Both STEMI and NSTEMI involve the release of specific myocardial necrosis markers.[2] Troponins are highly specific and sensitive biomarkers, while myoglobin serves as an early warning indicator for acute MI. Traditional markers, such as CK-MB and lactate dehydrogenase (LDH), are still used for the prognosis of acute MI.[3] Researchers are currently investigating novel, potentially useful biomarkers for STEMI diagnosis in clinical settings.[4] Therefore, it is imperative to identify new biomarkers for the rapid and accurate detection of myocardial injury.[5]

Traditional biomarkers incorporated into routine clinical practice, such as TNTs and the myoglobin percentage of creatine phosphokinase, correlate with patients' long-term outcomes after STEMI. TNT levels begin to rise in acute MI patients within 3.5 h of chest discomfort onset.[6] These biological markers of acute cardiac injury generally have low sensitivity and specificity, except for TNTs, particularly highly sensitive TNTs, in STEMI.[7]

Heart-specific circulating miR-1 has been identified as a marker of myocardial contractility loss and cardiomyocyte damage.[8] Additional research has shown that miR-1 is associated with circulating glucose in STEMI patients and may indicate heart damage in cardiogenic shock.[9] Studies have verified that upregulating miR-1 leads to an increase in *BCL2* protein expression. *BCL2*, a member of the *BCL2* family, can either promote or inhibit cell death.[10] Elevated *BCL2* expression has been reported to mitigate MI-related injury caused by high-dose feudal pre-treatment. Other studies have also demonstrated that *BCL2* protects against MI-induced damage.[11] The expression of the anti-apoptotic protein *BCL2*, a potential target of miR-1, is inversely related to miR-1 levels. Previous research indicates that increased miR-1 expression significantly contributes to cardiomyocyte death by post-transcriptionally suppressing *BCL2* expression. Therefore, reducing miR-1 expression could be a valuable strategy to prevent cardiomyocyte apoptosis.[12]

It has been demonstrated that circulating miRNA-126-5p expressed in the heart can be detected in all patient plasma within 4 h as an early indicator, whereas cardiac troponin is initially found in only 85% of patients.[13] miRNA-126-5p may therefore be a better biomarker in the early stages of AMI than cTnT.[14] miR-126-5p plays a multifaceted role in STEMI, primarily through its effects on endothelial function, angiogenesis, inflammation modulation, and the PI3K/AKT signaling pathway.[15] miR-126-5p can suppress genes such as PIK3R2 and mTOR at the transcriptional level and indirectly regulate EGFL7 isoform B.[16] According to earlier reports, miR-126-5p directly inhibits negative regulators of the VEGF pathway, including PIK3R2 (the PI3K regulatory subunit 2). The latent miR-126-5p target gene *PIK3R2* decreases the PI3K/AKT signaling pathway, which governs the growth and survival of multiple cell types.[17] The PI3K/AKT pathway is essential for controlling the development and survival of cells such as cardiomyocytes. Furthermore, activation of the PI3K/AKT pathway has been shown to reduce adverse post-infarct myocardial changes.[18] *PIK3R2* mRNA is directly targeted by miR-126-5p, leading to translational inhibition or mRNA degradation.[19] As a result, cardiomyocytes exhibit lower levels of the *PIK3R2* protein. Enhanced AKT activation supports tissue preservation during ischemic injury by promoting cell survival and reducing cardiomyocyte apoptosis.[20] Additionally, miR-126-5p promotes angiogenesis, thereby improving blood flow and facilitating tissue regeneration and post-infarction recovery. Overexpression of miR-126-5p strengthens protective signaling pathways in the heart, promoting healing and minimizing damage during STEMI.[21] This effect is achieved by targeting *PIK3R2* and diminishing its inhibitory influence on the PI3K/AKT pathway.[22,23]

Methodology

Retrieve structures of miRNA

With the accession number MIMAT0000416, the mature hsa-miR-1-3p is a thoroughly studied miRNA molecule. The hairpin structures hsa-miR-1-2 and hsa-miR-1-1 are its sources, and their sequence is UGGAAUGUAAAGAAGUAUGUAU. Experimental evidence supports its discovery and functional role in cellular processes, including cloning and Illumina sequencing.[24] Source: https://mirbase.org/mature/MIMAT0000416. The miR-1 structure was manually built using Pymol software (Figure 1A). RNA secondary structure modeling program like RNAfold (Vienna RNA Package) (https://mirbase.org/mature/MIMAT0000444) was used to identify the miR126-5p. The three-dimensional configurations of the molecules miR-1-3p and miR-126-5p are represented in Figure 1B.

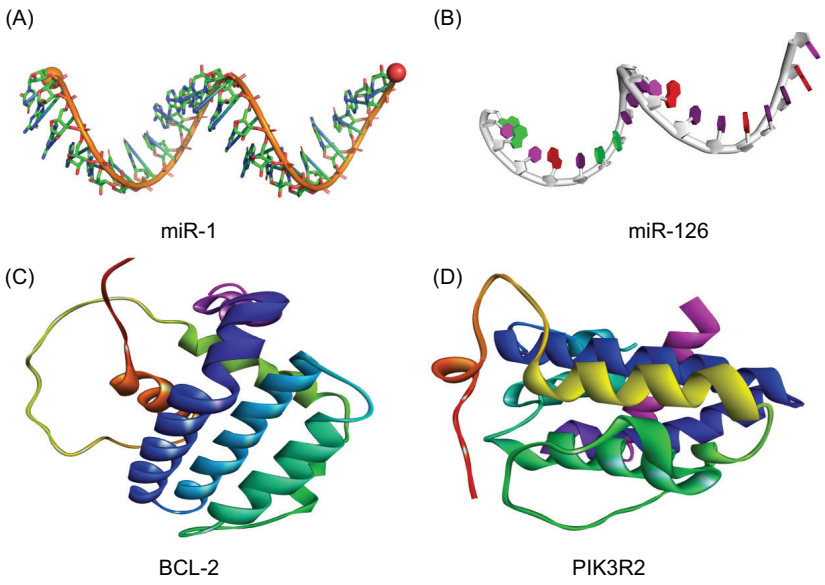

Figure 1 The 3D structure of miR-1, miR-126, *BCL2*, and *PIK3R2*.

Protein preparation

Scientific interest is focused on the protein Apoptosis regulator *BCL2*, encoded by the *BCL2* gene in the source organism *Homo sapiens* (human). The Protein Data Bank (PDB) (https://www.rcsb.org) provides the 3-dimensional crystallographic structures of proteins.[25] The 3D structures of BCL2 (pdb_00001g5m) and PIK3R2 (pdb_00002xs6) proteins were assessed. We downloaded the *BCL2* (Figure 1C) and *PIK3R2* (Figure 1D) 3D structures from the PDB, as represented in Figure 1. The protein structures were further analyzed using the PDBsum online tool, which revealed unique features, including helices.[26] Co-crystallized ligands and unnecessary water molecules were removed to prepare the proteins. Gasteiger charges and partial charges were then added at physiological pH to promote the protonation of polar hydrogens.[27]

Docking

Docking was done using HDOCK Server (http://hdock.phys.hust.edu.cn/), but before docking, we prepared both protein structure and miR-1 and miR-126 in 3D RNA format.[28] Using the HDOCK Server, we uploaded the miR-1 RNA structure and the *BCL2* protein structure for docking. Similarly, the miR-126 RNA structure and the *PIK3R2* protein structure were uploaded for docking. The docked complexes miR1-*BCL2* (Figure 2A) and miR126-*PIK3R2* (Figure 2B) are shown in Figure 2. After docking was completed, the resulting interaction files were downloaded in PDB format. We used PyMOL tools to visualize and analyze the docking interactions.[29] Interaction analyses provided by PDBsum were reviewed, including details on hydrogen bonds, hydrophobic interactions, and other non-covalent interactions. The PLIP server (https://projects.biotec.tu-dresden.de/plip-web) was used to examine the interacting amino acids and the bond distances between them.[30]

Sequence complementarity

Sequence complementarity was verified using tools such as TargetScan and miRanda, which identified potential binding sites with high alignment scores and significant free energy values, indicating strong interactions.[31] RNAhybrid and RNAfold predicted stable hybrid structures with low free energy values, supporting the likelihood of miRNA-mRNA binding. RNAcofold and mFold further confirmed that these interactions are thermodynamically favorable, showing low free energy and melting temperatures.

Study subjects

This cross-sectional study was conducted at the Institute of Molecular Biology and Biotechnology (IMBB), The University of Lahore (UOL), over a period of six months after obtaining ethical approval (Ref-IMBB/BBBC/24/005-B). Data were collected from 45 STEMI patients presenting to the ER of different hospitals in Punjab and from 45 controls aged 30-80 years, using convenient sampling after informed consent. Patients with a previous cardiac history were excluded. Socio-demographic information was recorded using a proforma. A 10 mL venous blood sample from each participant (volume varied depending on the condition) was drawn with a sterilized syringe for RNA isolation, Troponin T, and protein analysis, and collected separately into a 3 cc gel vial and an EDTA tube. Samples were centrifuged at 3000 rpm for 5 min at 4 °C. The resulting sera were stored at -80 °C until further use. A double volume of RNA solution was then added to the serum so that 2 mL of RNA solution was combined with 1 mL of blood serum as a preservative for RNA storage.

Isolation of miR1 and miR126

Serum was isolated from clotted blood by centrifuging whole blood after sample collection. miR-1 was extracted

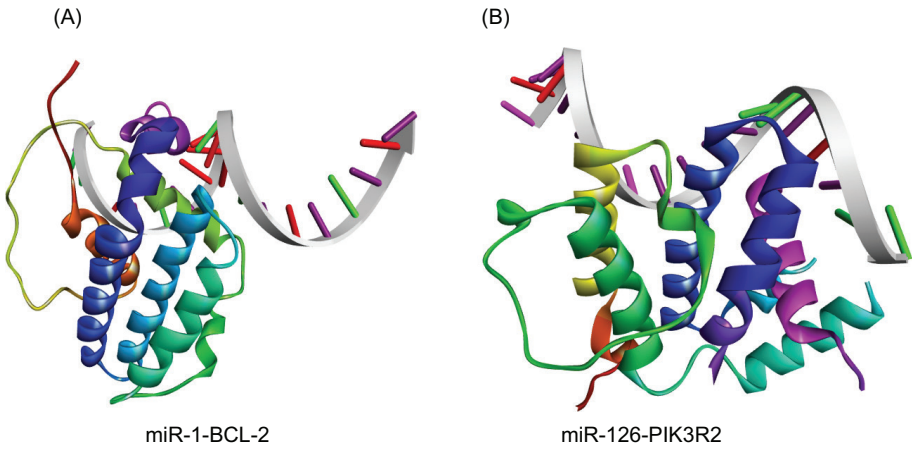

Figure 2 The 3D structure of *BCL2*-miR1, *PIK3R2*-miR126 docked complexes.

using the miRNA extraction kit "FavorPrep GEL/PCR Purification Mini Kit (100)" according to the manufacturer's instructions. miR-126-5p (0.5–0.7 μL) was also extracted using the miRNA isolation kit. The extracted miRNAs were purified through ethanol precipitation and column-based separation, followed by elution in release buffer. The quality of the recovered miRNAs was assessed using gel electrophoresis.

cDNA conversion

Extracted miRNAs (miR-1 and miR-126) were converted to cDNA using a reverse transcriptase GScriptultRA first-strand synthesis kit. Following the manufacturer's protocol, the template RNA was mixed with random hexamers and dNTPs, followed by reverse transcription with buffer, DTT, RNase inhibitors, and reverse transcriptase. The reaction mixture was incubated at the optimum temperature for cDNA synthesis. The resulting cDNA product was stored at -20 °C for PCR.

Quantification using qRT-PCR

Quantification of amplified cDNA was performed using SYBR Green dye. A quantitative reverse transcription-polymerase chain reaction (qRT-PCR) with SYBR Green master mix was used to quantify the levels of miR-1 and miRNA-126-5p.[32] The "Rotorgene 5000 Q" instrument operated with the "Rotor-Gene Q Software 2.3.5.1." Several critical steps were involved in the PCR process. A set of primers was designed to amplify each cDNA fragment (Table 1). qRT-PCR included an initial step at 95 °C for 12 min to activate the polymerase, followed by annealing and template extension steps of 20–30 s. For a total of 40 cycles, the annealing and extension temperatures were 60–65°C and 72°C, respectively. After PCR completion, the

Table 1 Representing docking score, Ligand score, Ligand RMSD, Interacting amino acids and H-A distance in the complexes.

Complex	Docking score	Ligand score	Ligand rmsd (Å)	Interacting Amino Acids	Distance-HA
BCL2-miR1	-251.49	0.8839	44.00	21A: TYR,	2.06
				25A: GLN,	2.26
				106A: ARG,	2.98
				107A: ARG,	2.62
				108A: TYR,	3.39
				143A: ASN,	3.32
				202A: TYR,	4.06
PI3K3-miR1s26	-207.15	0.7582	57.99	136A: GLU,	3.18
				227A: GLN,	2.89
				234A: ARG,	3.27
				240A: GLY,	2.12
				244A: ARG,	2.96
				285A: GLU,	3.01
				286A: LYS,	3.01
				289A: GLN,	2.12
				293A: GLU,	1.94

C_t method was used to compare the sample C_t values with those of standard samples. The housekeeping gene C_t values were used to normalize the C_t values of both samples and controls.

BCL2 apoptotic proteins were isolated and quantified using an Enzyme-Linked Immunosorbent Assay (ELISA). For this purpose, the *BCL2* ELISA kit was used, which was obtained from: https://www.bt-laboratory.com/index.php/Shop/Index/productShijiheDetail/p_id/1221/cate/kit.html.

PIK3R2 and hs-cTnT were isolated and quantitatively assessed using an Enzyme-Linked Immunosorbent Assay (ELISA). *PIK3R2* was measured using the Human Phosphatidylinositol 3-kinase Regulatory Subunit Beta, *PIK3R2* BT-LAB Kit, according to the manufacturer's instructions. hs-cTnT was assessed using the Human Troponin T, Cardiac Muscle, TNNT2 ELISA Kit BT-LAB. Statistical analysis was performed using Python, and results were presented as tables and figures, with a p-value < 0.05 considered significant.

Statistical analysis

Statistical analysis and data visualization in Python were performed by first uploading an Excel sheet using libraries such as pandas, which allow easy data import and manipulation.[33,34] All statistical analyses were conducted following machine learning method guidelines. After loading the dataset (e.g., using pd.read_excel('RSG.xlsx')), various analyses were performed using libraries like scipy, statsmodels, and numpy.[35] Descriptive statistics, including mean, median, standard deviation, and variance, were calculated using .describe() or numpy functions. To assess data distribution, the Shapiro-Wilk test was applied, which indicated that the data were not normally distributed. Non-parametric tests, such as the Mann-Whitney U test and Spearman correlation, were applied using SciPy. A linear regression model was used to determine correlations between variables. Visualization tools, including matplotlib and seaborn, facilitated graphical interpretation of data distributions and trends. This integrated approach enables comprehensive, reproducible, and customizable statistical analysis directly within the Python environment.

Results

Docking was performed using the HDOCK Server. The structures were uploaded, and the ligand scores of the miR-1-BCL2 (Figure 2A) and miR-126–PIK3R2 (Figure 2B) complexes were 0.89 and 0.76, respectively, indicating a strong association between the molecules. The resulting interaction files were downloaded in PDB format. To visualize and analyze interactions, the PDB files of the *BCL2* and *PIK3R2* complexes were loaded into PyMOL and saved. Understanding the molecular relationships between miR126-5p and the *PIK3R2* gene is essential for elucidating their potential roles in myocardial infarction. The interaction complexes are stabilized by hydrogen bonding, as shown in Table 1 and Figure 3. Strong base-pairing interactions are suggested by the high alignment scores and low free energy values provided by miRanda and RNAhybrid. The likelihood of robust miRNA–mRNA interactions is supported by thermodynamic stability and consistent secondary structure predictions across multiple tools. TargetScan's Context++ scores indicate that miR126-5p is a potentially effective *PIK3R2* regulator, as lower scores correspond to greater efficacy. These bioinformatics findings suggest that miR126-5p may regulate gene expression by interacting with the 3' UTR of the *PIK3R2* gene with considerable sequence complementarity and thermodynamic stability. The gene and primer sequences are presented in Table 2.

The mean ± S.D. age of cases and controls was 44.24 ± 11.0 and 34.4 ± 6.91 years, respectively. Among the participants, 25 (55.5%) were male and 20 (44.4%) were female. The mean ± S.D. body mass index (BMI) in cases and controls was 28.16 ± 2.07 and 27 ± 3.54, respectively. General symptoms associated with STEMI were also recorded (Table 3). Among the cases, 10 (30%) were smokers and 35 (70%) were non-smokers, whereas among the controls, 2 (8%) were smokers and 33 (92%) were non-smokers. The mean systolic blood pressure in cases and controls was 146.9 ±

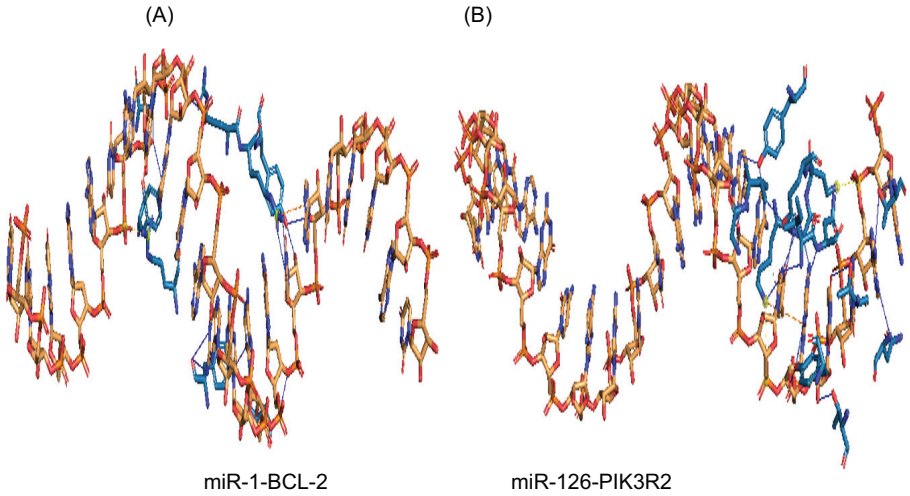

Figure 3 The complex representing the interactions, shown with dotted lines.

Table 2 Primer and Gene Sequences of hsa-miR-1-3p, HAS-miR-126-5p and U6.

	Forward Primer Sequence	Reverse Primer Sequence
hsa-miR-1-3p	5′-TGGAATGTAAAGAAGT-3′	5′-ATCCAGTGCAGGGTCCGAGG-3′
HAS-miR- 126-5p	5′ACAGTTCTCTCGTACCGTGAG TAAT3′	5′-AAAGGTTGATCTGCTCTCTCTCTC-3′
Gene	**Gene Forward Primer**	**Gene Reverse Primer**
U6	5′-CTCGCTTCGGCAGCACATAT ACT-3′	R, 5′-ACGCTTCACGAATTTGCGTGTC-3′

Table 3 General symptoms associated with STEMI.

Symptoms/Signs	STEMI (n=45)
Chest pain	18 (40%)
Sweating	14 (31%)
Shortness of breath	10 (22%)
Arm pain	08 (17.7%)
Epigastric discomfort	06 (13.3%)
Chest tightness/pressure	06 (13.3%)
Nausea and vomiting	05 (11.1%)
Fatigue and weakness	04 (8.88%)
Jaw and neck pain	03 (6.66%)

16.50 mmHg and 111.8 ± 10.82 mmHg, respectively, while the mean diastolic blood pressure was 95 ± 10.15 mmHg in cases and 72.4 ± 8.70 mmHg in controls.

The mean value of *PIK3R2* protein in cases was 228.55 ± 127.4, compared to 505.27 ± 66.6 in controls, showing a significant difference (p-value <0.005) between the study groups. The Relative Expression (Fold Change) formula, 2ΔCt, was used to compute the miR-126-5p values, where $\Delta C_t = C_t$ of microRNA − C_t of U6. The mean value of miR-126-5p in cases and controls was 0.17 ± 0.32 and 0.78 ± 1.33, respectively. Results indicated that the expression level of miR-126-5p is significantly correlated (p-value 0.003) with the prognosis of ST-elevated myocardial infarction. The mean cTNT among cases (0.77 ± 0.67) and controls (0.02 ± 0.01) showed significant differences (p-value <0.001) between the groups. The expression levels of *PIK3R2* and miR-126-5p demonstrated that the severity of ST-elevated myocardial infarction can be significantly correlated (p-value <0.005) with gene-to-protein expression levels (Table 4). The differential expression of miR-1 and miR-126-5p, as indicated by C_t values, is shown in Figures 6 and 7 for the STEMI and control groups. In the STEMI group of 45 individuals, *BCL2* levels ranged from 21.70 to 721.70, with a mean of 128.0111 and a standard deviation of 137.19194, demonstrating high variability around the mean. The control group, also comprising 45 individuals, had *BCL2* levels ranging from 10.70 to 93.70, with a mean of 40.6587 and a lower standard deviation of 20.92479 (Table 4). These findings highlight the variations in *BCL2* biomarker levels between the two groups, providing valuable insights into the molecular mechanisms underlying MI and emphasizing the significance of *BCL2* in understanding heart health and potential disorders such as STEMI. Figure 4 represents the levels of *BCL2* in control and STEMI groups, while Figure 5 represents the *PIK3R2* levels in controls and STEMI.

The Shapiro-Wilk Test Statistic showed a value of 0.58, with a p-value of 4.83×10^{-8} (p-value <0.005), indicating that the data is not normally distributed. The Mann-Whitney U Test was applied to a dataset containing *BCL2* levels and *PIK3R2* levels among STEMI patients, yielding a statistic of 167.0 with a p-value of 2.959×10^{-5} (p-value <0.005). This indicates a significant difference between the *BCL2* antibody and *PIK3R2* levels, as determined by the Mann-Whitney U test. The Spearman Correlation Coefficient was 0.611, demonstrating a significant correlation between *BCL2* antibody and *PIK3R2* using Spearman correlation. The levels of *BCL2* antibody and *PIK3R2* in STEMI are shown in Figure 8. Linear regression evaluation revealed a Mean Squared Error of 158743.74, an R^2 score of 0.8494, and a Mean Absolute Error of 239.8. The linear regression model, represented in Figure 9, demonstrated a significant correlation between the two proteins. Multiple comparisons between all pairs of proteins in STEMI were performed using Tukey's test, showing significant correlations in each pair, as illustrated in Figure 10.

Table 4 Levels of miR-126-5p, miR-1 and PIK3R2, BCL2 in Controls and C1ases.

	In Controls			In Cases		
	n	**Mean**	**Std. Deviation**	**n**	**Mean**	**Std. Deviation**
miR-126-5p	45	0.78	1.33	45	0.17	0.32
PIK3R2	45	505.27	66.6	45	228.55	127.4
miR-1	45	43.43	31.28	45	31.35	68.89
BCL2	45	40.66	20.92	45	128.01	137.19
Total	90			90		
p-value		<0.001			<0.005	

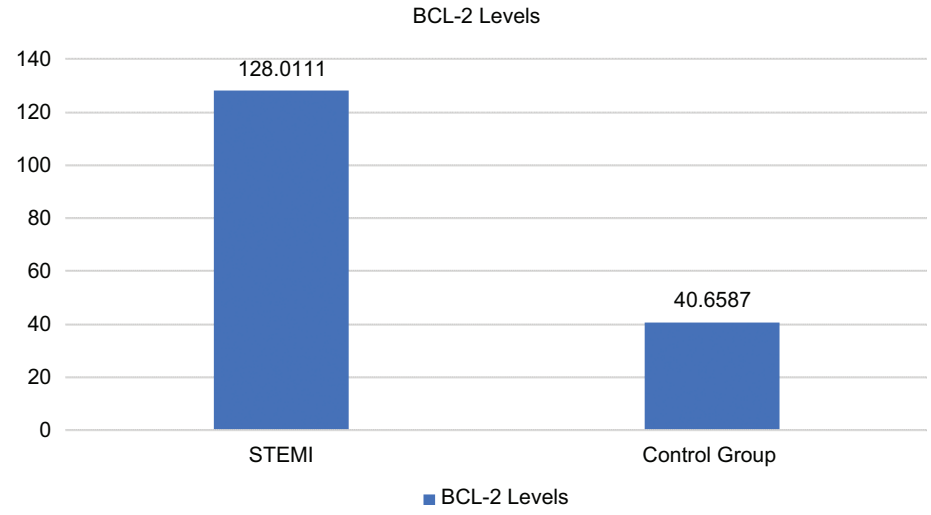

Figure 4 Mean levels of *BCL2* among cases and controls.

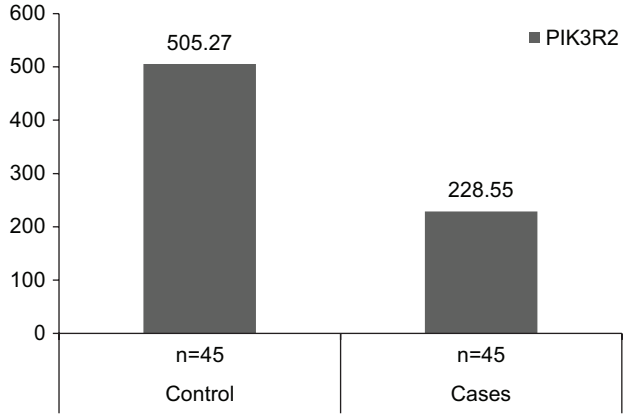

Figure 5 Mean levels of PIKER2 among cases and controls.

Discussion

The current study involves clinical research with human participants, specifically those with STEMI, and expands our understanding of the therapeutic potential of modifying the expression of miR-1 in relation to *BCL2* and miR-126-5p in relation to *PIK3R2*, which could contribute to the development of novel methods for the early detection of STEMI. The STEMI sample included 45 individuals aged 28 to 74, with a mean age of 44.24 years, while the control group had a mean age of 34.4 years. Both the STEMI and control groups consisted of 25 men and 20 women. The 45 STEMI participants had an average BMI of 28.16 with an S.D. of 2.07, whereas the control group had an average BMI of 27 with an S.D. of 3.54. The findings indicated that, compared to controls, STEMI patients were more obese. In obese

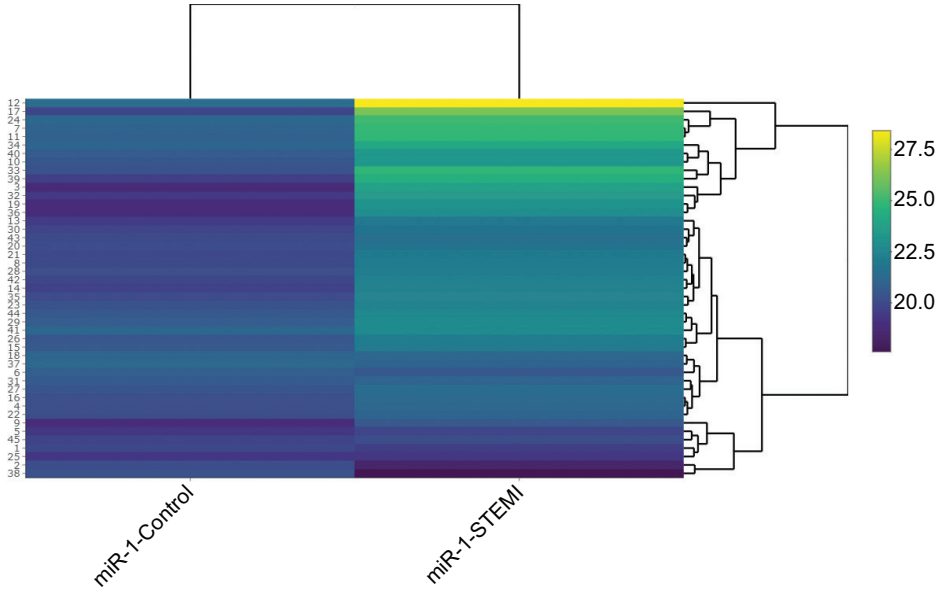

Figure 6 Differential expression of miR-1, as indicated by Ct values, between STEMI and Control.

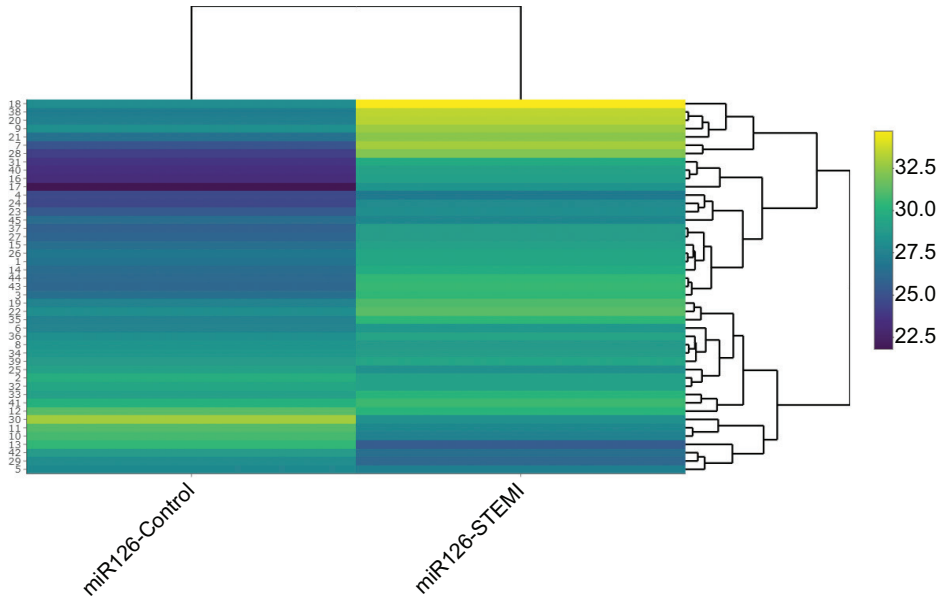

Figure 7 Differential expression of miR-126-5p, as indicated by Ct values, among STEMI and Control Samples.

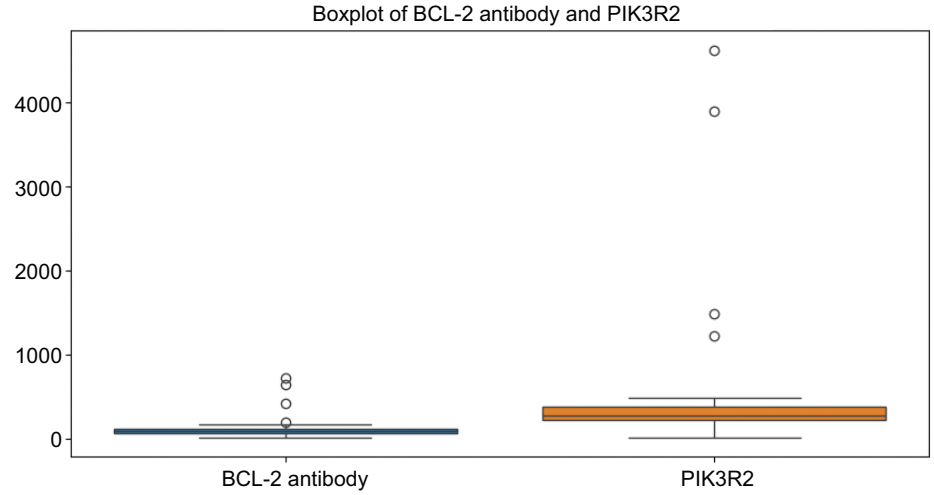

Figure 8 Expression levels of *BCL2* and PIK3R3 among STEMI.

patients, STEMI occurred earlier in life; the first STEMI event in obese patients happened three years earlier than in normal-weight patients (62.5 vs. 65.7 years, $p < 0.0001$). In summary, obesity is a risk factor for earlier manifestation of STEMI compared to normal-weight individuals and is associated with a trend toward decreased mortality in the subsequent clinical course after STEMI.[14]

The 45 STEMI participants in the current study had cTnT levels with a mean of 0.77 and an S.D. of 0.67. In contrast, the control group had cTnT levels with a mean of 0.02 and an S.D. of 0.01. The total ROC-AUC values for heart-type fatty acid-binding protein, creatine kinase MB, and hs-cTnT were 0.810, 0.716, 0.782, and 0.880, respectively, in different studies. For patients hospitalized more than 120 minutes after onset, the hs-cTnT diagnostic sensitivity and negative predictive value were both 100%. However, over the entire time frame, the specificity was limited.[15]

In the current study, *BCL2* levels in the STEMI group of 45 participants had a mean of 128.0111 and a standard deviation of 137.19, indicating significant variance around the mean. The control group, which also comprised 45 individuals, had *BCL2* levels with a mean of 40.6587 and a lower S.D. of 20.92479. In a related study, Sun et al. (2016) investigated the effects of miR-21 expression on the *BCL2*/caspase-3 and IL-6/STAT3 pathways in acute MI, showing that individuals with MI express higher levels of miR-21 than normal volunteers. Overexpression of miR-21 may enhance *BCL2* protein expression while inhibiting STAT3 protein expression.[36] Maclay prospectively included consecutive MI patients undergoing primary PCI, with 29 patients aged 67 ± 12 and 83% males treated for acute MI. Early growth response protein 1 and *BCL2* demonstrated a significant correlation ($r = 0.657$, $p < 0.001$). Patients with non-STEMI-ACS exhibited lower BCL2 *expression than those*

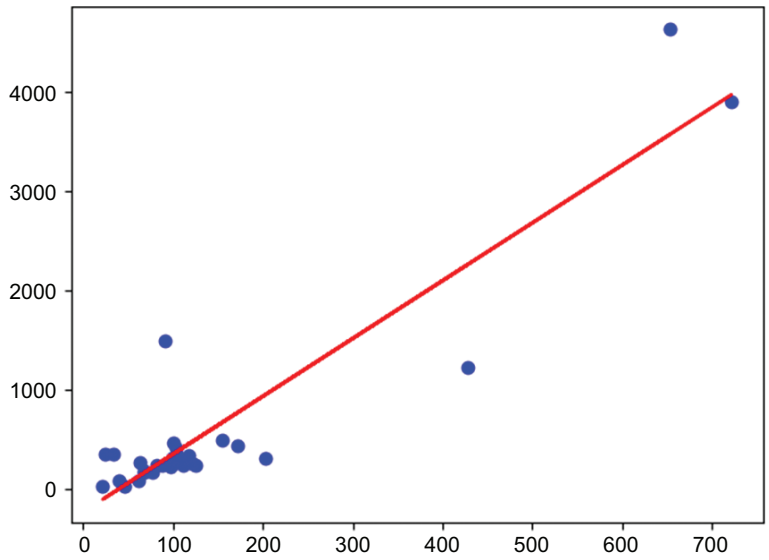

Figure 9 Linear regression model of *BCL2*(X-axis) and PIK3R3(Y-axis) among STEMI.

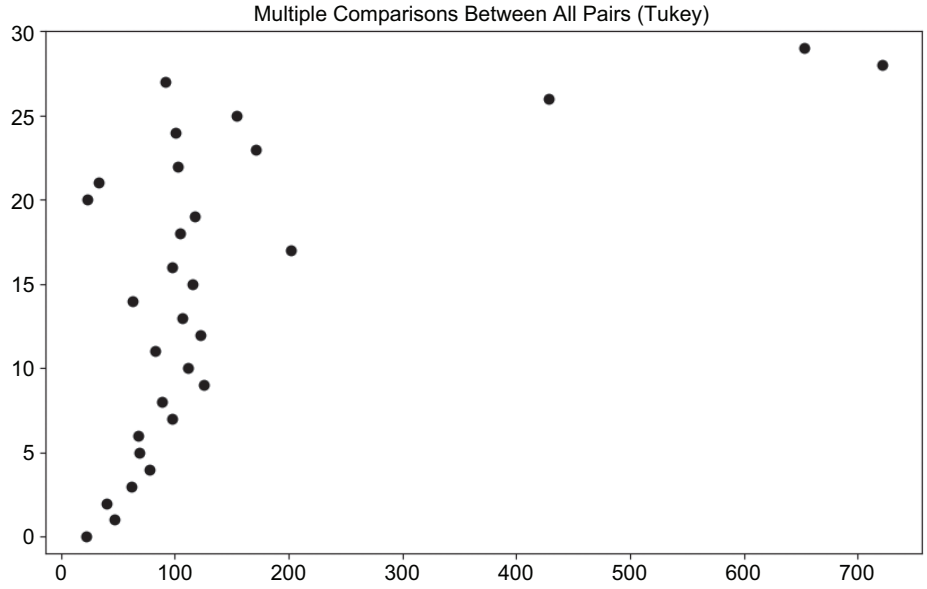

Figure 10 Multiple comparisons between each pair of BCL2 and PIK3R3 proteins among STEMI.

with STEMI-ACS (2.7 ± 1.2 vs. 4.8 ± 1.0, p = 0.001). In the current investigation, miRNA levels for 90 samples from each group were calculated using the Relative Expression technique. The STEMI group had a mean C_t value of 31.353 with a standard deviation of 68.895, and C_t values ranged from 0.102 to 324.034. The control group's C_t values ranged from 6.105 to 156.498, with a mean of 43.431 and a standard deviation of 31.285.

When a patient presents to the ED with suspected AMI, 6–22% exhibit minor increases in hs-cTnT/I. The addition of 1h-hs-cTn alterations significantly improves the early detection of AMI compared to copeptin.[37] In the current investigation, the STEMI group of 45 individuals showed *PIK3R2* levels with a mean of 228.55 and an S.D. of 127.4, indicating substantial variation around the mean. The 45-person control group had PIK3R2 levels with a mean of 505.27 and a lower S.D. of 66.6. Relative quantification of miR-126-5p in 45 STEMI patients revealed a mean of 0.17 with an S.D. of 0.32, while the control group showed a mean serum miR-126-5p level of 0.78 with an S.D. of 1.33. In a previous study, the vascular group (i.e., the IR-ATO and IR-BVR groups) exhibited a significantly higher relative expression of miR-126 (2.667 ± 0.1045) compared to the control group (1.04 ± 0.04034). Infarct-related artery total occlusion AMI, as opposed to vascular-incomplete AMI, may be diagnosed using miR-126. These findings support further research and clinical application of circulating miR-21-5p and miR-126 as IR-ATO AMI diagnostic biomarkers.[38]

The suppression of *BCL2* by miR-1 suggests a direct pro-apoptotic role, as *BCL2* is a key anti-apoptotic regulator that preserves mitochondrial membrane integrity and prevents cytochrome c release. In the current study,

the results indicated a clear discrepancy in *BCL2* levels, which were significantly higher in STEMI patients, as well as lower miRNA-1 concentrations compared to the control group. This aligns with earlier evidence that elevated miR-1 levels are associated with myocardial injury and apoptosis in cardiac tissues. These findings suggest a critical function for miRNA-1 in regulating *BCL2* expression, potentially affecting cardiomyocyte survival during STEMI episodes. Furthermore, the discussion highlighted the potential of targeting the miR-1/*BCL2* axis as an effective treatment method for controlling STEMI. Similarly, a comparison of the association of miR-126-5p with its target protein *PIK3R2* revealed that the average of miR-126-5p is 0.17 with an S.D. of 0.32 in 45 STEMI patients, and the average of *PIK3R2* is 228.55 with an S.D. of 127.4. The interaction of miR-126-5p with PIK3R2 is functionally significant in angiogenesis and endothelial repair. PIK3R2 encodes the regulatory subunit of PI3K, which modulates PI3K/AKT signaling, a central pathway in endothelial survival, migration, and neovascularization. It has been previously revealed that miR-126 targets *PIK3R2*, which encodes the p85β regulatory subunit of PI3K.[39,40] Both genes regulate cardiomyocyte survival—PIK3C3 through autophagy and *BCL2* through apoptosis inhibition. These mechanistic insights connect our in-silico work with expression analysis data and functional outcomes. Our in-silico data showed strong binding affinities of these miRNAs with *BCL2* and PIK3R2 proteins, predicting an effect of these miRNAs. The expression analysis data of these miRNAs, with the functional outcomes of these proteins, confirmed their regulatory role and strong association with STEMI.

An imbalance, such as decreased PIK3C3 activity and increased BCL2 levels during STEMI, can exacerbate myocardial injury. The statistical analysis showed that both proteins are correlated in STEMI and have a strong association with the disease. We conclude that the crosstalk between autophagy and apoptosis, mediated by PIK3C3 and *BCL2*, is a critical determinant of cell fate in myocardial infarction.

Conclusion

The study's findings indicate that BCL2 levels are significantly higher in STEMI patients, presumably serving as a compensatory mechanism to prevent cell death. The lower levels of miR-1 in STEMI patients imply that miR-1 may have a role in the etiology of STEMI, presumably by driving cardiomyocyte death. This work sheds light on the possible functions of miR-1 and *BCL2* in STEMI patients. The study concluded that *PIK3R2* levels were lower in STEMI patients than in controls. This highlights the particular significance of miR-126-5p, which targets the PIK3R2 protein during STEMI and activates the PI3K/Akt pathway, thereby regulating downstream factors in cell proliferation, angiogenesis, and apoptosis across diverse cell types. The expression of miR-126-5p in patients indicates that it may be helpful for the early diagnosis of STEMI by activating the PI3K/Akt pathway, which is involved in the regulation of angiogenesis by targeting the *PIK3R2* protein. However, this cross-sectional study is limited by its small cohort size; further longitudinal and larger cohort studies, along with functional validation experiments, are needed to fully understand the complicated dynamics of this disorder and to develop advanced therapies for its treatment.

Ethical Approval

The ethical approval for this study was granted by Ethical Review Committee Institute of Molecular Biology and Biotechnology, The University of Lahore (UOL) under refernce no (IMBB/BBBC/24/005-B) dated 05/01/2024.

Author's Contribution

Conceptualization, Madeeha Shahzad Lodhi; methodology, Arshia Mehmood; software, Almas Muhammad Arshad; validation, Nawal Al-Hoshani and Shaza N. Alkhatib; formal analysis, Hafiza Saba Safdar; investigation, Tahir Maqbool; resources, Awais Altaf; data curation, Omniah A. Mansouri and Hanan Abdulrahman Sagini.; writing—original draft preparation, Muhammad Faisal.; writing—review and editing, Maher S Alwethaynani; visualization, Hanan Abdulrahman Sagini; supervision, Awais Altaf and Madeeha Shahzad Lodhi.; project administration, Madeeha Shahzad Lodhi; funding acquisition, Awais Altaf.

Conflict of Interest

The authors declare no conflict of interest.

Funding

The authors are thankful to Princess Nourah bint Abdulrahman University Researchers Supporting Project number (PNURSP2026R437), Princess Nourah bint Abdulrahman University, Riyadh, Saudi Arabia

References

1. Vogel B, Claessen BE, Arnold SV, Chan D, Cohen DJ, Giannitsis E, et al. ST-segment elevation myocardial infarction. Nature. 2019;5(1):39. https://doi.org/10.1038/s41572-019-0090-3
2. Xue S, Liu D, Zhu W, Su Z, Zhang L, Zhou C, et al. Circulating MiR-17-5p, MiR-126-5p and MiR-145-3p are novel biomarkers for diagnosis of acute myocardial infarction. Front. 2019;10:123. https://doi.org/10.3389/fphys.2019.00123
3. Danese E, Montagnana MJAotm. An historical approach to the diagnostic biomarkers of acute coronary syndrome. Ann Transl Med. 2016;4(10):194. https://doi.org/10.21037/atm.2016.05.19
4. Tanase DM, Gosav EM, Ouatu A, Badescu MC, Dima N, Ganceanu-Rusu AR, et al. Current knowledge of MicroRNAs (miRNAs) in acute coronary syndrome (ACS): ST-elevation myocardial infarction (STEMI). Life. 2021;11(10):1057. https://doi.org/10.3390/life11101057
5. Amezcua-Guerra B, Amezcua-Castillo LM, Guerra-López JA, Díaz-Domínguez KA, Sánchez-Gloria JL, Cruz-Melendez A, et al. Diagnostic performance of serum MicroRNAs for ST-segment elevation myocardial infarction in the emergency department. Biomedicines. 2023;11(9):2422. https://doi.org/10.3390/biomedicines11092422

6. Christenson E, Christenson RH. The role of cardiac biomarkers in the diagnosis and management of patients presenting with suspected acute coronary syndrome. Ann Lab Med. 2013 Aug 8;33(5):309. https://doi.org/10.3343/alm.2013.33.5.309
7. Fan Y, Chen Y, Wan Z, Zhou D, Ma AJJoCM. The prognostic value of autoantibodies against ß1-adrenoceptor and cardiac troponin-I for clinical outcomes in STEMI. JCM. 2017;18(1):34-41. https://doi.org/10.2459/JCM.0000000000000273
8. Kazimierczyk E, Eljaszewicz A, Kazimierczyk R, Tynecka M, Zembko P, Tarasiuk E, et al. Altered microRNA dynamics in acute coronary syndrome. Adv Interv Cardiol. 2020;16(3):287-93. https://doi.org/10.5114/aic.2020.99263
9. Kura B, Kalocayova B, Devaux Y, Bartekova MJIjoms. Potential clinical implications of miR-1 and miR-21 in heart disease and cardioprotection. Int J Mol Sci. 2020;21(3):700. https://doi.org/10.3390/ijms21030700
10. Tang Y, Zheng J, Sun Y, Wu Z, Liu Z, Huang GJIhj. MicroRNA-1 regulates cardiomyocyte apoptosis by targeting Bcl-2. Int Heart J. 2009;50(3):377-87. https://doi.org/10.1536/ihj.50.377
11. Korshunova AY, Blagonravov ML, Neborak EV, Syatkin SP, Sklifasovskaya AP, Semyatov SM, et al. BCL2-regulated apoptotic process in myocardial ischemia-reperfusion injury. IJMM. 2021;47(1):23-36. https://doi.org/10.3892/ijmm.2020.4781
12. Wang L, Yuan Y, Li J, Ren H, Cai Q, Chen X, et al. MicroRNA-1 aggravates cardiac oxidative stress by post-transcriptional modification of the antioxidant network. Cell Stress Chaperones. 2015;20(3):411-20. https://doi.org/10.1007/s12192-014-0565-9
13. Wang X, Zhang X, Ren X-P, Chen J, Liu H, Yang J, et al. MicroRNA-494 targeting both proapoptotic and antiapoptotic proteins protects against ischemia/reperfusion-induced cardiac injury. Circulation. 2010;122(13):1308-18. https://doi.org/10.1161/CIRCULATIONAHA.110.964684
14. Creemers EE, Tijsen AJ, Pinto YMJCr. Circulating microRNAs: novel biomarkers and extracellular communicators in cardiovascular disease. Circ Res. 2012;110(3):483-95. https://doi.org/10.1161/CIRCRESAHA.111.247452
15. Sharma AK, Bisht P, Gupta B, Akhtar MS, Alavudeen SS, Afzal O, et al. Investigating miRNA subfamilies: can they assist in the early diagnosis of acute myocardial infarction. Drug Discov Today. 2023;28(10):103695. https://doi.org/10.1016/j.drudis.2023.103695
16. Zhang X, Yang Y, Li Y, Zhang W, Song XJDO. miR-126-5p suppresses HeLa and Ishikawa cell proliferation and migration via the RICTOR/AKT pathway. Discov Oncol. 2025;16(1):533. https://doi.org/10.1007/s12672-025-02306-8
17. Tang X, Chen Y, Luo H, Bian Q, Weng B, Yang A, et al. miR-126 controls the apoptosis and proliferation of immature porcine sertoli cells by targeting the pik3r2 gene through the PI3K/AKT signaling pathway. Animals. 2021;11(8):2260. https://doi.org/10.3390/ani11082260
18. Walkowski B, Kleibert M, Majka M, Wojciechowska MJC. Insight into the role of the PI3K/Akt pathway in ischemic injury and post-infarct left ventricular remodeling in normal and diabetic heart. Cells. 2022;11(9):1553. https://doi.org/10.3390/cells11091553
19. Han B, Chu C, Su X, Zhang N, Zhou L, Zhang M, et al. N6-methyladenosine-dependent primary microRNA-126 processing activated PI3K-AKT-mTOR pathway drove the development of pulmonary fibrosis induced by nanoscale carbon black particles in rats. Nanotoxicology. 2020;14(1):1-20. https://doi.org/10.1080/17435390.2019.1661041
20. Xiaoyu L, Wei Z, Ming Z, Guowei JJCT. Anti-apoptotic effect of MiR-223-3p Suppressing PIK3C2A in cardiomyocytes from myocardial infarction rat through regulating PI3K/Akt signaling pathway. Cardiovasc Toxicol. 2021;21(8):669-82. https://doi.org/10.1007/s12012-021-09658-x
21. Laura Francés J, Pagiatakis C, Di Mauro V, Climent MJB. Therapeutic potential of EVs: targeting cardiovascular diseases. Biomed. 2023;11(7):1907. https://doi.org/10.3390/biomedicines11071907
22. Qu M-J, Pan J-J, Shi X-J, Zhang Z-J, Tang Y-H, Yang G-YJNN. MicroRNA-126 is a prospective target for vascular. Neurol Neuroimmunol Neuroinflamm. 2018;5:1-7. https://doi.org/10.20517/2347-8659.2018.01
23. Li S-N, Li P, Liu W-H, Shang J-J, Qiu S-L, Zhou M-X, et al. Danhong injection enhances angiogenesis after myocardial infarction by activating MiR-126/ERK/VEGF pathway. Biomed Pharmacother. 2019;120:109538. https://doi.org/10.1016/j.biopha.2019.109538
24. Neri M, Fabbri M, D'Errico S, Di Paolo M, Frati P, Gaudio RM, et al. Regulation of miRNAs as new tool for cutaneous vitality lesions demonstration in ligature marks in deaths by hanging. Sci Rep. 2019;9(1):20011. https://doi.org/10.1038/s41598-019-56682-7
25. Jin X, Awale M, Zasso M, Kostro D, Patiny L, Reymond J-LJBb. PDB-Explorer: a web-based interactive map of the protein data bank in shape space. BMC bioinformatics. 2015;16(1):339. https://doi.org/10.1186/s12859-015-0776-9
26. Laskowski RA, Jabłońska J, Pravda L, Vařeková RS, Thornton JMJPs. PDBsum: Structural summaries of PDB entries. Protein Sci. 2018;27(1):129-34. https://doi.org/10.1002/pro.3289
27. Singh RP, Singh RN, Srivastava AK, Kumar S, Dubey R, Arora DKJJoASiES. Structural analysis and 3d-modelling of fur protein from bradyrhizobium japonicum. J. Appl Sci Environ Sanit. 2011;6(3).
28. Yan Y, Zhang D, Zhou P, Li B, Huang S-YJNar. HDOCK: a web server for protein–protein and protein–DNA/RNA docking based on a hybrid strategy. NAR. 2017;45(W1):W365-W73. https://doi.org/10.1093/nar/gkx407
29. Yuan S, Chan HS, Hu ZJWIRCMS. Using PyMOL as a platform for computational drug design. Comput mol sci. 2017;7(2):e1298. https://doi.org/10.1002/wcms.1298
30. Schake P, Bolz SN, Linnemann K, Schroeder MJNAR. PLIP 2025: introducing protein–protein interactions to the protein–ligand interaction profiler. NAR. 2025:gkaf361. https://doi.org/10.1093/nar/gkaf361
31. Creighton CJ, Nagaraja AK, Hanash SM, Matzuk MM, Gunaratne PHJR. A bioinformatics tool for linking gene expression profiling results with public databases of microRNA target predictions. RNA. 2008;14(11):2290-6. https://doi.org/10.1261/rna.1188208
32. Lu S-J, Ma M-Y, Yan X-G, Zhao F-J, Hu W-Y, Ding Q-W, et al. Development and application of a low-priced duplex quantitative PCR assay based on SYBR Green I for the simultaneous detection of porcine deltacoronavirus and porcine sapelovirus. Vet Med. 2023;68(3):106. https://doi.org/10.17221/79/2022-VETMED
33. Sial AH, Rashdi SYS, Khan AHJIJ. Comparative analysis of data visualization libraries Matplotlib and Seaborn in Python. IJATCSE. 2021;10(1):277-81. https://doi.org/10.30534/ijatcse/2021/391012021
34. McKinney W. Python for data analysis: Data wrangling with Pandas, NumPy, and IPython: O'Reilly Media, Inc.; 2012. 385.
35. Hill C, Du L, Johnson M, McCullough BJWIRDM, Discovery K. Comparing programming languages for data analytics: Accuracy of estimation in Python and R. WIREs. 2024;14(3):e1531. https://doi.org/10.1002/widm.1531
36. Sun H, Cai J, Xu L, Liu J, Chen M, Zheng M, et al. Expression of miR-21 is involved in myocardial infarction through the IL-6/STAT3 and Bcl-2/caspase-3 pathway. IJCEP. 2016;9:2795-802.
37. Boeddinghaus J, Reichlin T, Nestelberger T, Twerenbold R, Meili Y, Wildi K, et al. Early diagnosis of acute myocardial infarction in patients with mild elevations of cardiac troponin. Clin Res Cardiol. 2017;106(6):457-67. https://doi.org/10.1007/s00392-016-1075-9

38. Mi X-l, Gao Y-p, Hao D-j, Zhang Z-j, Xu Z, Li T, et al. Prognostic value of circulating microRNA-21-5p and microRNA-126 in patients with acute myocardial infarction and infarct-related artery total occlusion. Front cardiovasc med. 2022;9:947721. https://doi.org/10.3389/fcvm.2022.947721
39. Wu Q, Qi B, Duan X, Ming X, Yan F, He Y, et al. MicroRNA-126 enhances the biological function of endothelial progenitor cells under oxidative stress via PI3K/Akt/GSK3β and ERK1/2 signaling pathways. BJBMS. 2021;21(1):71. https://doi.org/10.17305/bjbms.2019.4493
40. Zhang M, Hamblin MH, Yin K-JJNi. Long non-coding RNAs mediate cerebral vascular pathologies after CNS injuries. Neurochem Int. 2021;148:105102. https://doi.org/10.1016/j.neuint.2021.105102